IEEE Access
Multidisciplinary ⋮ Rapid Review ⋮ Open Access Journal

Received September 16, 2020, accepted October 2, 2020, date of publication October 12, 2020, date of current version October 22, 2020.

Digital Object Identifier 10.1109/ACCESS.2020.3030188

Coalition Formation Games for Coordinated Service in Realistic Small Cell Propagation Topologies

PANAGIOTIS GEORGAKOPOULOS[1], (Member, IEEE), LOIZOS KANARIS[2], TAFSEER AKHTAR[1], (Graduate Student Member, IEEE), AKIS KOKKINIS[2], STAVROS STAVROU[3], (Member, IEEE), AND ILIAS POLITIS[1], (Member, IEEE)

[1]Wireless Communications Laboratory, University of Patras, 26504 Patras, Greece
[2]Research and Development Department, Sigint Solutions Ltd., 2311 Nicosia, Cyprus
[3]Faculty of Pure and Applied Sciences, Open University of Cyprus, 2220 Nicosia, Cyprus

Corresponding author: Panagiotis Georgakopoulos (pgeorgako@ece.upatras.gr)

This work was supported by the European Union's Horizon 2020 Research and Innovation Programme under the Marie Skłodowska-Curie under Grant Agreement H2020-MSCA-RISE-2016-SONNET-734545 and Agreement H2020-MSCA-ITN-SECRET-722424.

ABSTRACT The densification of modern wireless networks into a dense ecosystem of small cells imposes challenges for the reliable service and high quality of experience of its users as it can result into severe intercell interference, especially for users scattered on the cell edges. Joint Transmission Coordinated Multipoint (JT-CoMP) is a technique that can be deployed to form cooperating clusters of transmission points, enabling them to jointly transmit data to significantly mitigate this type of interference for these users. However, JT-CoMP stresses the backhaul links and radio resources are limited, meaning that, with incautious clustering, the data rates for cell edge users may not improve, while the data rates for the non-cell edge users may severely decrease. To tackle these drawbacks, a dynamic coalition formation algorithm is proposed to form the appropriate transmission point clusters to implement JT-CoMP. Furthermore, to ensure reliable service for all the network's users, the case where JT-CoMP is enhanced with the capability to serve users based on their selected application is examined. The proposed scheme's adaptability and capability to increase cell edge user throughput is then tested and compared to the non JT-CoMP case, a JT-CoMP scheme with static clustering and a JT-CoMP scheme with greedy clustering for a user mobility scenario. To obtain more reliable and accurate results of the JT-CoMP deployment, physical layer parameters retrieved from a fully deterministic physical layer radio planning tool (TruNET wireless) are imported for our simulations.

INDEX TERMS 5G, coalition formation games, C-RAN, interference coordination, resource management, self-organizing networks, small cells.

I. INTRODUCTION

The emergence of the fifth generation (5G) wireless networks aims to satisfy the ever-growing demands of mobile users by providing them with increased data rates and ultra-reliable low-latency provision of a certain level of communication services [1]. Additionally, the technical requirements of 5G include the service of 10 to 100 times more connected devices compared to existing technologies [2].

An appropriate strategy to meet these requirements is the densification of the network in key areas, where cells of different coverage are planned to be co-deployed in high traffic indoor and outdoor propagation environments, creating a multi-tier heterogeneous network of small cells and increasing the network capacity [3]. This means that flexible radio resource allocation strategies, which strive for a fair distribution of the available radio resources to a plethora of connected devices, need to be adopted [4], [5]. Furthermore, these strategies must have the ability to adapt to continuous network changes, as multiple users constantly move from one cell to another, changing the traffic load and meddling with the wireless channel of other users.

Cloud radio access networks (C-RAN) are considered a key enabler for small cell deployment. In C-RAN, unlike

The associate editor coordinating the review of this manuscript and approving it for publication was Francisco Rafael Marques Lima.

traditional architectures, the radio unit, called Remote Radio Head (RRH), and the processing unit, called Base Band Unit (BBU), are separated. Furthermore, the main idea behind C-RAN is to co-locate multiple BBUs into a centralized location, forming a virtualized BBU pool for statistical multiplexing gain [6]. Additionally, C-RAN can severely reduce the small cell realization cost by lowering the number of BBUs in densely deployed heterogeneous small cell networks and enhance their energy efficiency while reducing their power consumption [7].

The deployment of multiple neighbouring small cells can dramatically increase the interference that a user receives from other cells, i.e. the intercell interference. This type of interference is especially increased for users located in cell edges, preventing them from receiving their requested level of quality of service (QoS). Downlink Coordinated Multipoint (CoMP) is a strategy that can be adopted to address this problem [8]. CoMP in the downlink can be distinguished into two main techniques, coordinated scheduling/beamforming CoMP and joint processing CoMP. These cooperation techniques aim to avoid or exploit interference in order to improve the cell edge user data rates. Specifically, for Joint Transmission CoMP (JT-CoMP), a subclass of joint processing CoMP, the same data channel is simultaneously transmitted from multiple cooperating transmission points to the same cell edge user equipment (UE) by using the same radio resources, i.e. Resource Blocks (RBs). Therefore, the intercell interference can be mitigated by converting an interfering signal from another cell to a desired signal. C-RAN can efficiently support advanced features such as CoMP and interference mitigation as multiple BBUs can coordinate with each other to share the scheduling information, channel status and user data efficiently to improve the system capacity as well as reduce interference in the system [7]. In this study, only JT-CoMP will be examined.

The clustering of cooperating transmission points in JT-CoMP has been identified as a significant challenge in various studies [8], [9]. Besides feedback overhead and backhaul traffic, in wireless systems with limited resources, when JT-CoMP is activated, there is a possibility of committing too many resources to cell edge UEs (or edge UEs), especially if their percentage in the formed clusters is high. As shown in our previous studies, [10], [11], this could result in severely reduced spectral efficiency and data rates for the UEs not in the cell edges (or non-edge UEs), while edge UEs may also not receive sufficient RBs to increase theirs. A game theoretic clustering approach based on coalition formation games was selected and compared to a static clustering approach where the only criterion to form a coalition was the distance between the transmission points. Coalition formation games account for network structure and the costs of cooperation, while satisfying the individual rational demands of the network nodes [12], which is why clustering based on this method was selected in [10], [11] and is also adopted in this study. However, in this study, we implement some additional rules and conditions to examine scenarios with user mobility and additional user data rate needs due to their application.

Regarding the notations used in this article, lowercase or uppercase letters refer to scalars, boldface lowercase letters denote vectors and boldface uppercase letters denote matrices. Furthermore, the superscripts $(\cdot)^T, (\cdot)^H, (\cdot)^{-1}, (\cdot)^\dagger$ denote the transpose, the conjugate transpose, the matrix inverse and the Moore-Penrose pseudo-inverse respectively. Additionally, $|\cdot|$ and $||\cdot||$ indicate the norm and the Euclidean norm of a scalar and vector respectively.

II. BACKGROUND AND CONTRIBUTION

A. RELATED STUDIES

A significant amount of work has been dedicated to studying various techniques of cooperative transmissions for interference mitigation in wireless communication systems. In [13], base station coordination with dirty paper coding was initially proposed with single-antenna transmitters and receivers in each cell. In [14], joint transmissions with cooperative base stations for downlink multi-cell multi-user MIMO networks are explored for intercell interference mitigation. The proposed schemes include a dirty paper coding approach with perfect data and power cooperation among base stations with a pooled power constraint and several sub-optimal joint transmission schemes with per-base power constraints. However, the clustering of base stations and large scale simulations with orthogonal resource allocation are not considered.

CoMP has been proposed and studied as a solution for interference coordination in several studies [8], [15], [16]. Specifically, in [16], the JT-CoMP technique has been shown to be capable of providing the highest gains in terms of cell capacity in dense homogeneous and heterogeneous cell deployments among the various CoMP schemes. However, several challenges for its effective implementation have been identified by these studies, including the cell clustering and backhaul capacity and latency constraints.

Regarding clustering in CoMP, various research papers consider static clustering methods [17]–[19]. However, dynamic solutions capable of being effective in scalable scenarios and capable to respond to changing network conditions to maximize CoMP gains are required. In [20], an overlapping dynamic clustering scheme with a greedy search algorithm is proposed. This solution requires high computational complexity when large network size is considered, and thus, lacks scalability. In [21], a dynamic cluster formation algorithm is presented which merges cells into clusters based on the total improvement in spectral efficiency and all users' SINR. However, the algorithm lacks scalability and the improvement in individual user data rate is not considered. Also, backhaul capacity constraints and possible costs of cooperation are not taken into account. In [22], CoMP multi-user multiple-input-and-multiple-output (MU-MIMO) downlink transmissions are examined, where the clustering is performed in multiple steps based on backhaul constraints as well as radio properties for one UE served by each base station. The study showed that the CoMP gain by increasing cluster size

becomes much less or even negligible if backhaul constraints are considered. In [23], the authors examine a joint dynamic base station clustering and beamformer design problem in a network where Joint Processing CoMP is deployed in the downlink by formulating and solving a non-convex max-min rate problem. The main aim of this study is to maximize the minimum rate among all users and limit the cooperating cluster size without hurting the achievable common rate. However, realistic channel parameters and possible resource scarcity for the UEs are not considered. In [24], a dynamic CoMP clustering algorithm is presented, aiming to maximize group average SINR under the constraint of maximum target cell blocking probabilities for group communications in Mission-Critical Communications. The authors consider a dynamic traffic model and analyze the trade-off between high SINR and network capacity. As in many other works, individual mobile user performance in terms of throughput is not considered for the base station clustering. In [25], a user-centric CoMP clustering algorithm for maximizing the users' spectral efficiency, given a maximum cluster size, is presented. The algorithm is then enhanced to balance the load across the small cells and improve user satisfaction and a two-stage reclustering algorithm is presented. However, the complexity of the algorithm increases with the increase of the number of users and small cells.

A number of recent studies focus on implementing non-cooperative and cooperative game theory for the transmission point clustering in order to achieve interference mitigation in downlink transmissions as it can provide distributed solutions with reduced signalling overhead and consider possible cooperation costs. In [26], a coalition formation game is modeled to cluster the small cell base stations so that they can perform cooperative beamforming to mitigate the effects of intercell interference and shadow fading. In [27], [28] a coalition formation game is formulated to form cooperation clusters to mitigate intercell interference and improve user performance via Time-Division Multiple Access (TDMA) based transmissions. However, in these studies, JT-CoMP or the parallel service of all the UEs are not considered. In contrast with [25], a load-aware network-centric clustering algorithm is presented in [29], where load balancing and spectral efficiency objectives are jointly optimized through a coalition formation game based on merge and split operations in a JT-CoMP downlink heterogeneous network scenario. The algorithm accounts for various overhead costs and is capable of dynamically adjusting the cluster size to adapt to different network load. As in [25], realistic channel parameters were not considered and clustering changes are proposed over longer time intervals meaning that small-scale phenomena are not considered. Furthermore, the proposed algorithm in [29] aims to form coalitions based on total utility improvement, ignoring possible individual payoff reductions. A study that compares static, dynamic distributed and dynamic game theoretic clustering approaches can be found in [30]. The dynamic distributed clustering algorithm was found to provide the most improvement in terms of user throughput. However, the algorithm is not designed to account for cooperation costs, individual player payoff improvements or reductions are not considered in the game theoretic solution since its objective is to increase a total utility and JT-CoMP is not deployed.

B. MOTIVATION AND CONTRIBUTION

As discussed in Section I, increased intercell interference is a major drawback for user performance in small cell systems. This problem can be addressed with cooperative transmissions via JT-CoMP. However, JT-CoMP is not guaranteed to increase the edge users' performance when the radio resources are limited and the clustering is incautious. Furthermore, backhaul constraints have to be taken into consideration. For this purpose, coalition formation games can be utilized for the self-organization of transmission points into coalitions as they account for costs of cooperation. Additionally, it is of particular interest to study scenarios where user mobility and time-varying channels are taken into account. Thus, a dynamic coalition formation game has to be formulated as these scenarios impose changes to the game's nature by activating handovers and changing the traffic load of the transmission points.

To accurately study the proposed scheme's impact it is extremely significant to provide system level simulations with realistic wireless propagation modeling, where multiple users, competing for radio resources, are simultaneously served. More specifically, the contributions of this study can be summarized as follows:

1) A distributed low-complexity dynamic coalition formation algorithm was developed and tested in a small-cell interference heavy environment, where multiple users were served simultaneously, aiming to form the appropriate JT-CoMP clusters for maximizing the individual throughput of each edge UE, without severely undermining the throughput of the rest, while a backhaul constraint was satisfied.
2) Suitable utility and individual payoff functions were formulated, making the representation of edge UEs from the cooperating transmission points, i.e. the RRHs, possible in the coalition formation game.
3) Output from a fully deterministic, physical layer simulator (TruNET wireless) was imported and used for the calculations of Vienna LTE-A Downlink System Level Simulator, creating an accurate and reliable method for system level simulations.
4) JT-CoMP was enhanced with the capability to account for the individual needs of users for extra data rate, according to their selected application.
5) The performance in terms of throughput for a moving UE, in addition to the ability of our proposed algorithm to adapt in a dynamically changing network, was tested.

   As supported by the extracted results, the effectiveness of our approach was confirmed for all the use cases.

III. SYSTEM MODEL

A homogeneous C-RAN based small cell network consisting of L RRHs in the access network is assumed, where OFDMA is the selected multiple access scheme and the RRHs are assumed to have omnidirectional coverage, forming L total cells. We focus on the downlink transmission where the L total RRHs of the network serve a total of K UEs each, accounting for $L \cdot K$ total UEs in the network. The available frequency spectrum is divided into R subcarriers, while in every Transmission Time Interval (TTI) each RRH has N_{RB} Resource Blocks (RBs) available to serve its attached UEs. Let $\mathcal{L} = \{1,\ldots,l,\ldots,L\}$ represent the set of RRHs, while $\mathcal{K}_l = \{1,\ldots,k,\ldots,K\}$ represents the set of each cell's UEs. All the UEs are equipped with N_r antennas, while the RRHs are equipped with N_t omnidirectional antennas.

Prior to the transmission over the wireless channel, the user symbol vector $\boldsymbol{x}_{k,l,r}$ is precoded with a precoding matrix $\boldsymbol{W}_{k,l,r} \in \mathbb{C}^{N_t \times n_{k,l}}$, selected from the LTE codebook [31], mapping the $n_{k,l}$-dimensional transmit symbol vector onto the N_t antennas, where $n_{k,l}$ is the number of data-streams spatially multiplexed to user k, with $n_{k,l} \leq \mathrm{N_r}$. Also, the allocation of the available transmit power is considered in the precoding matrices.

For the r-th subcarrier, the N_r-dimensional received signal vector of UE k, served by RRH l can be expressed by the following formula:

$$\boldsymbol{r}_{k,l,r} = \boldsymbol{H}_{k,l,r}\boldsymbol{W}_{k,l,r}\boldsymbol{x}_{k,l,r} + \sum_{i=1,\neq l}^{L} \boldsymbol{H}_{k,i,r}\boldsymbol{W}_{\xi,i,r}\boldsymbol{x}_{\xi,i,r} + \boldsymbol{z}_{k,l,r} \tag{1}$$

where, $\boldsymbol{H}_{k,l,r} \in \mathbb{C}^{N_r \times N_t}$ is the total MIMO channel matrix describing the channel between UE k and RRH l and $\boldsymbol{z}_{k,l,r} \in \mathcal{N}_{\mathbb{C}}\left(0, \sigma_z^2 I_{N_r}\right)$ is the Additive White Gaussian Noise (AWGN) added at the receiver. The second term of the equation represents the intercell interference caused by transmissions from other RRHs in the network (noted i) to other UEs (noted ξ) at the r-th subcarrier. Also, it is assumed that the transmit symbol vector is normalized as:

$$\mathbb{E}\left[\boldsymbol{x}_{k,l,r}\boldsymbol{x}_{k,l,r}^H\right] = \boldsymbol{I}_{n_{k,l}} \tag{2}$$

where, $\boldsymbol{I}_{n_{k,l}}$ is the identity matrix sized $n_{k,l}$.

The users are assumed to employ a Minimum Mean Square Error (MMSE) filter to equalize their respective channels and to separate spatially multiplexed data-streams from each other and from the interference caused by the transmission to other users. To compute their receive filters, perfect feedback is assumed at all the receivers, i.e. the UEs. The $n_{k,l} \times N_r$ dimensional receive filtering matrix applied to user k in cell l, is written as $\boldsymbol{G}_{k,l,r}$. Applying this matrix to the received signal vector, the estimated symbol vector is obtained as:

$$y_{k,l,r} = \boldsymbol{G}_{k,l,r}\boldsymbol{H}_{k,l,r}\boldsymbol{W}_{k,l,r}\boldsymbol{x}_{k,l,r} + \sum_{i=1,\neq l}^{L} \boldsymbol{G}_{k,l,r}\boldsymbol{H}_{k,i,r}\boldsymbol{W}_{\xi,i,r}\boldsymbol{x}_{\xi,i,r} + \boldsymbol{G}_{k,l,r}\boldsymbol{z}_{k,l,r} \tag{3}$$

The MMSE receive filter is expressed as:

$$\boldsymbol{G}_{k,l,r} = \left(\left(\boldsymbol{\Gamma}_{k,l,r}\right)^H \boldsymbol{\Gamma}_{k,l,r} + \sigma_z^2 \boldsymbol{I}_{n_{k,l}}\right)^{-1} \left(\boldsymbol{\Gamma}_{k,l,r}\right)^H \tag{4}$$

where,

$$\boldsymbol{\Gamma}_{k,l,r} = \boldsymbol{H}_{k,l,r}\boldsymbol{W}_{k,l,r} \tag{5}$$

Assuming the described MMSE filter on the receiver side, the post equalization SINR for the k-th UE which is served by the l-th RRH, for the stream $v \in [1,\ldots, n_{k,l}]$, at the r-th subcarrier is expressed by the following formula:

$$SINR_{k,l,r,v} = \frac{\left|\boldsymbol{g}_{k,l,r,v}^H \boldsymbol{H}_{k,l,r}\boldsymbol{w}_{k,l,r,v}\right|^2}{I_{intercell} + I_{self} + \sigma_z^2\left|\boldsymbol{g}_{k,l,r,v}\right|^2} \tag{6}$$

where,

$$I_{intercell} = \sum_{i=1,\neq l}^{L} |\boldsymbol{g}_{k,l,r,v}^H \boldsymbol{H}_{k,i,r}\boldsymbol{W}_{\xi,i,r}|^2 \tag{7}$$

$$I_{self} = \sum_{\mu=1,\neq v}^{n_{k,l}} |\boldsymbol{g}_{k,l,r,v}^H \boldsymbol{H}_{k,l,r}\boldsymbol{w}_{k,l,r,\mu}|^2 \tag{8}$$

At equations (6)-(8), $\boldsymbol{g}_{k,l,r,v}$ and $\boldsymbol{w}_{k,l,r,v}$ denote the v-th column of $\boldsymbol{G}_{k,l,r}^H$ and $\boldsymbol{W}_{k,l,r}$ respectively. The useful signal power of stream v is represented by the numerator, while the denominator includes the intercell interference power from other RRHs that operate at the same frequency, given by equation (7), self-interference caused by other user streams, given by equation (8), and the noise power. The symbols of different users are assumed as statistically independent. Single User Multiple Input Multiple Output (SU-MIMO) is assumed, so the in-cell interference between the spatially multiplexed streams is ignored on the formulas.

After the per-subcarrier and per-stream post equalization SINR is extracted, MIESM (Mutual Information Effective Signal to Interference and Noise Ratio Mapping) [32] is employed to calculate an effective SINR value via compressing the corresponding post equalization SINR values of the assigned RBs, yielding an AWGN-equivalent representation in terms of mutual information, in order to determine the CQI and the MCS. This single effective SINR value is then be further mapped to a BLER (Block Error Ratio) value. After that, the size of the Transport Block can be determined according to the LTE standards and an instantaneous throughput value can be obtained for the current TTI.

The UEs are divided into two categories based on their effective SINR, edge and non-edge UEs. For a non-edge user, the previously described equations apply for their SINR and throughput calculation. When a UE is considered edge, it can be served by multiple cooperating RRHs which can form a JT-CoMP coalition Π_s. We define $\mathcal{P} = \{\Pi_1, \Pi_2,\ldots, \Pi_s,\ldots, \Pi_S\}$ as the set or collection of coalitions in the network. In this case, the composite total channel matrix $\boldsymbol{H}_{k,l,r}$ is calculated by stacking the matrices from each transmitter $c \in [1,\ldots, C]$ in the coalition, as in [33], i.e.,

$$\boldsymbol{H}_{k,l,r} = \left[\boldsymbol{H}_{k,l_1,r}, \ldots, \boldsymbol{H}_{k,l_C,r}\right] \epsilon \mathbb{C}^{N_r \times CN_t} \tag{9}$$

Then, the effective channel matrix is calculated as $\boldsymbol{H}_{eff^{k,l,r}} = \boldsymbol{G}_{k,l,r}\boldsymbol{H}_{k,l,r}\boldsymbol{W}_{k,l,r}$. This effective channel does not become available to the simulator until run-time. This means that the optimal precoders and the corresponding receive filters cannot be calculated a-priori. In this case, the optimal precoder $\boldsymbol{W}_{k,l,r}$ and the corresponding receive filter $\boldsymbol{G}_{k,l,r}$ are calculated at runtime using the simulator's *run-time-precoding* method [33].

The per-subcarrier and per-stream post equalization SINR for edge UE k_e which is served by cluster Π_s is expressed by the following equation:

$$SINR_{k,l,r,v} = \frac{\left|\boldsymbol{g}^H_{k_e,l,r,v}\boldsymbol{H}_{k_e,l,r}\boldsymbol{w}_{k_e,l,r,v}\right|^2}{I_{intercell} + I_{self} + \sigma_z^2\left|\boldsymbol{g}_{k_e,l,r,v}\right|^2} \tag{10}$$

where,

$$I_{intercell} = \sum_{i=1,\notin\Pi_s}^{L} \left|\boldsymbol{g}^H_{k_e,l,r,v}\boldsymbol{H}_{k_e,i,r}\boldsymbol{W}_{\xi,i,r}\right|^2 \tag{11}$$

$$I_{self} = \sum_{\mu=1,\neq v}^{n_{k,l}} \left|\boldsymbol{g}^H_{k_e,l,r,v}\boldsymbol{H}_{k_e,l,r}\boldsymbol{w}_{k_e,l,r,\mu}\right|^2 \tag{12}$$

Then, an effective SINR value is extracted using MIESM and the throughput of the UE is calculated based on the LTE specifications. It is evident by observing equations (10) and (11) that the more RRHs in a coalition, the more the numerator of equation (10) increases, while the denominator decreases, resulting in a higher edge UE post equalization SINR value.

IV. PROBLEM FORMULATION

In this section, the proposed coalition formation game will be defined and formulated, after we formulate our maximization problem.

This study's motivation is the improvement of the edge UEs' performance in terms of throughput. Our selected way of improving the edge UEs' performance is the implementation of JT-CoMP. In a system with limited resources (i.e. the RBs) this improvement is inevitably accomplished at the expense of the non-edge UEs' throughput. It is clear that a set of constraints need to be set in order to achieve fair resource allocation and a performance balance for all the devices in the network. These constraints include a maximum throughput decrease for the non-edge UEs and a backhaul capacity constraint, as in JT-CoMP the same data need to be simultaneously present at all the transmission points that serve an edge UE, resulting in a potentially huge backhaul load. Therefore, our maximization problem is formulated as follows:

$$max \sum_{l=1}^{L} R_{k_e,l} \tag{13}$$

$$s.t.: \; R_{k_n,l} > R'_{k_n,l}(1-\alpha), \quad \forall k_n \tag{14}$$

$$T \leq T_{thres} \tag{15}$$

where, $R_{k_e,l}$ is the throughput of an edge UE k_e which is initially served by the l-th RRH, $R_{k_n,l}$ is the throughput of the non-edge UE k_n served by the l-th RRH after a new coalition is formed and JT-CoMP is activated, $R'_{k_n,l}$ is its throughput before the coalition formation game begins, assumed constant for the whole duration of the game, and α ($0 \leq \alpha \leq 1$) is the maximum acceptable percentage of its decrease. Finally, T is the backhaul capacity which must not exceed a limit T_{thres} and is calculated as in [34].

JT-CoMP mitigates the intercell interference of the edge UEs by forming cooperating clusters of transmission points, also referred to as coalitions. By forming coalitions, the interfering signals of neighbouring RRHs can be treated as desired signal resulting into increased SINR and data rate. This is clearly indicated by equation (11) and is a strong incentive for any transmission point to belong in a coalition. However, the implementation of JT-CoMP carries some drawbacks. As shown at [11], incautious clustering of RRHs with many attached edge UEs can result in significantly lower throughput for non-edge UEs, while the throughput of the edge UEs may not always improve due to limited RBs to allocate when their RRH has to allocate RBs to a large number of UEs. Therefore, intelligence needs to be behind the coalition formation to guarantee a throughput improvement for all edge UEs and a moderate throughput reduction for the non-edge UEs. Contrary to traditional clustering methods, such as the formation of static clusters only based on the inter-site (or inter-RRH in our case) distance, we developed a coalition formation game in which the players (i.e. the transmission points) form coalitions to solve the optimization problem defined in equations (13)-(15). Coalition formation games are an attractive approach to address drawbacks of collaborative scenarios in wireless communication networks as they account for cooperation costs [12] and enable the independent and strategic decision making of network nodes and devices [35].

Hence, our formulated game is a coalition formation game with non-transferable utility (NTU), defined by a pair $(\mathcal{L}, U)$, where $\mathcal{L}$ presents the finite set of players and U as a characteristic function which associates with every coalition $\Pi_s \subseteq \mathcal{L}$ a set of payoff vectors.

Although JT-CoMP benefits the individual throughput of edge UEs in the network, its implementation demands the formation of coalitions consisting of RRHs. This means that the players in our proposed coalition formation game are the RRHs and a function that captures the throughput changes for each user of an RRH when it is participating in a coalition Π_s has to be formulated. A suitable function for this purpose, referred to as payoff function of $\text{RRH}_l \in \Pi_s$, is given by:

$$\phi_l(\Pi_s) = A_l - (E_l - 1 - q_{e,l} + d_{e,l}) - (N_l - 1 - q_{n,l} + d_{n,l}) + \phi'_l \tag{16}$$

and

$$A_l = \sum_{k_e=1}^{E_l} sgn(R_{k_e,l} - R'_{k_e,l}) + \sum_{k_n=1}^{N_l} sgn(R_{k_n,l} - \beta R'_{k_n,l}) \tag{17}$$

where $\mathcal{E}_l = [1, \ldots, k_e, \ldots, E_l]$ represents the set of edge UEs and $\mathcal{N}_l = [1, \ldots, k_n, \ldots, N_l]$ represents the set of non-edge UEs at the l-th RRH respectively and $\beta = 1 - \alpha$. Intonations were used for values of previous partitions that satisfied the game's conditions, while $R'_{k_n,l}$ represents always the throughput of non-edge UE k_n before the game starts. Also, $q_{e,l}$ and $d_{e,l}$ account for the number of edge UEs with intact and decreased throughput respectively, before and after Π_s is tested, while $q_{n,l}$ and $d_{n,l}$ represent the number of non-edge UEs with equal and less throughput respectively compared to their individual threshold, after Π_s. Finally, in equation (17), the sign function was used where:

$$sgn(R^b - R^a) = \begin{cases} -1, & R^b < R^a \\ 0, & R^b = R^a \\ 1, & R^b > R^a \end{cases} \tag{18}$$

When at least one edge UE's throughput decreased or one non-edge UE's throughput decreased below its corresponding threshold by examining a coalition, the three first terms of equation (16) yield a negative value, indicating that Π_s is not beneficial for the RRH. If both conditions are satisfied, the payoff of the RRH increases, indicating that the coalition is beneficial for the throughput of its edge UEs while the throughput of its non-edge UEs is not severely undermined. Therefore, the game can be played on behalf of the UEs, while the RRHs are considered the players.

Finally, we define the utility function of coalition Π_s as:

$$U(\Pi_s) = \begin{cases} V(\Pi_s), & T \leq T_{thres} \\ 0, & T \geq T_{thres} \end{cases} \tag{19}$$

and:

$$V(\Pi_s) = \sum_{l \in \Pi_i} \phi_l(\Pi_s) \tag{20}$$

When, the backhaul capacity exceeds T_{thres}, $U(\Pi_s)$ becomes zero, indicating that the coalition Π_s is not beneficial for the network.

By observing equations (7) and (11), it is clear that the intercell interference for both the edge and non-edge users is not depended on how the players in $\mathcal{L} \backslash \Pi_s$ are structured, but only on their overall number, thus, our game is in characteristic form. Also, for two disjoint coalitions $\Pi_c \subset \mathcal{L}$ and $\Pi_d \subset \mathcal{L}$, $U(\Pi_c \cup \Pi_d)$ may not always be greater than $U(\Pi_c) + U(\Pi_d)$ due to possible non-edge UEs' throughput reduction below their threshold or possible edge UEs' throughput reduction which can result in decreased payoff values for the involved RRHs and decreased utility when $\Pi_c \cup \Pi_d$. Therefore, our formulated game is non-superadditive, meaning that the coalition of all the network's RRHs (grand coalition) may not be the optimal structure [35].

V. PROPOSED COALITION FORMATION ALGORITHM

In this section, our proposed coalition formation **Algorithm 1** for the self organization of the RRHs in coalitions will be introduced. We assume that the mobile users can move for the duration of the game. This imposes changes to the game's nature, as moving UEs can be attached to different RRHs by activating handovers, while changing their traffic load. Moreover, propagation channels are dynamic, resulting in varied effective SINRs for the UEs, which can cause changes in their edge or non-edge status. Therefore, a dynamic coalition formation algorithm needs to be constructed that can adapt to possible changes. For this purpose, we adopted the same coalition formation algorithm based on merge and split operations that was used in [10], [11] with an extra restriction on the maximum coalition size and two additional external rules to adapt to user mobility, explained in Section VI, that enable its reactivation. The merge and split operations are based on the Pareto order, meaning that between two collections of coalitions with the same players, one is preferred to another if at least one player improves its payoff, while the payoff of the other players is not decreased. Our proposed coalition formation algorithm is divided in three stages:

1) Initially, the small cell network consists of L total non-cooperating RRHs, referred to as singleton coalitions. Each RRH l serves E_l edge UEs and N_l non-edge UEs.
2) A search of potential coalition patterns among RRHs begins as soon as, all users are scheduled and receive interference from the neighboring singleton RRHs. Each edge UE calculates the carrier-to-interference (or C/I) ratio values between its serving and interfering RRHs and fills an $(L-1) \times 1$ vector consisting of these values. The interfering RRHs are assigned a unique ID by each user and this ID is forwarded to the C-RAN. In case the RRHs are serving multiple edge UEs, the proposed functionality at the C-RAN, averages their values, resulting in L total interference vectors. Then, after these vectors are sorted in ascending order, based on their carrier-to-interference values, they are combined into an $(L-1) \times L$ carrier-to-interference matrix $\boldsymbol{I}_M$.
   Then, the values on the first row of $\boldsymbol{I}_M$ are compared and a priority list is extracted, indicating the order in which each RRH will seek a cooperator, alongside with a candidate list, consisting of the IDs of each RRH's interferers. Essentially, the priority list indicates the order in which each coalition combination between the most interfering RRHs will be tested.
3) In the third stage, all possible coalitions, indicated by the priority and candidate lists, are tested for a duration of 10 TTIs and their members are coordinated based on the JT-CoMP technique. A coalition among two or more interfering RRHs is formed (merging functionality) if a set of constrains is satisfied, otherwise the existing clusters remain intact. Firstly, the tested coalition increases (or at least does not decrease) the throughput of every edge UE. Secondly, the throughput of the non-edge UEs is not decreased below a certain threshold value set beforehand. Thirdly, the backhaul capacity constraint is satisfied. All these conditions are

Algorithm 1 Proposed Coalition Formation Algorithm

1: **Initial Stage**:
The network consists of L singleton coalitions.
2: **Priority List Formation Stage**:
for all edge UEs **do**
Calculate the C/I values from all the interferers.
end for
for all $l \in \mathcal{L}$ **do**
if attached edge UEs ≥ 2 **then**
Average their edge UEs' C/I values.
end if
end for
Form the C/I matrix $\boldsymbol{I}_M$.
3: **Coalition Formation Stage**:
for every row of $\boldsymbol{I}_M$ **do**
Extract the row's C/I values.
Form the priority and candidate lists.
Extract the examined pairs $\boldsymbol{O}$ from the priority and candidate lists.
if all extracted C/I values $\leq C/I_{threshold}$ **then**
(a)
for every $l \in \boldsymbol{O}$ **do**
calculate $\phi_l(\Pi_s)$
if $\phi_l(\Pi_s)$ increases via Pareto order, $U(\Pi_s)$ increases and coalition size $\leq$ max coalition size **then**
Merge.
end if
end for
(b)
for every $s \in S$ **do**
for every $l \in \Pi_s$ **do**
calculate $\phi_l(\Pi_j)$ after split, where Π_j a singleton coalition
if $\phi_l(\Pi_j)$ increases via Pareto order **then**
Split.
end if
end for
end for
end if
end for

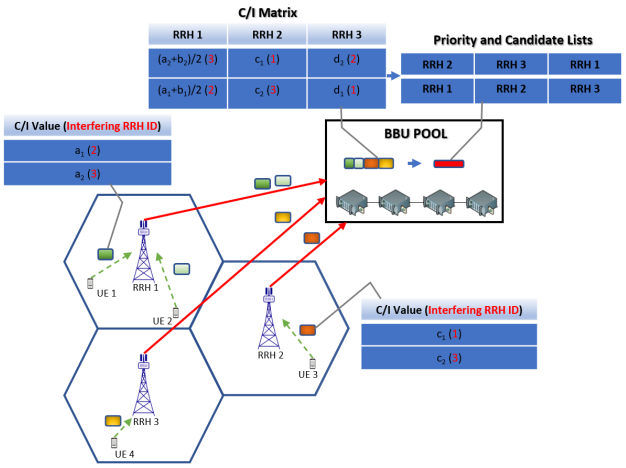

FIGURE 1. Priority list formation procedure.

represented by the payoff of an RRH and the utility function of a coalition, i.e equations (16) and (19). Moreover, to guarantee limited feedback overhead, a maximum coalition size threshold is implemented.
If a coalition has already been tested, then, the next one (based on the priority list) is examined. However, when new priority and candidate lists are extracted, previously examined coalitions can be tested again, since the formation of a previously rejected coalition can be favoured over time due to user mobility. Also, if an RRH is already a member of a coalition and its turn, based on the priority list, comes, then the total coalition between the new candidate and all the existing members of the coalition is tested. All the information about the coalition formation game, e.g. the record of attempted coalitions, the IDs of the RRHs inside a tested coalition, the throughput values for each UE of the involved RRHs before and after a coalition is tested, is kept in the proposed C-RAN functionality.
Following this process, the next row of $\boldsymbol{I}_M$ is considered, and a new priority and candidate list is made. This stage will be repeated until all the considered values of the interference matrices exceed the predefined C/I threshold, in which case the game ends. A formed coalition will split (splitting functionality) only when this spit results into the increase of the payoff of at least one member RRH, while the payoffs of the other RRHs do not decrease.

An example of the procedure to form the priority and candidate lists is depicted in Fig. 1. In this example, the C-RAN network consists of three RRHs and four edge UEs. RRH 1 serves UE 1 and UE 2, while RRH 2 serves UE 3 and RRH 3 serves UE 4. To form the lists, each UE sends their calculated C/I vector via their serving RRH to the cloud. For example, the C/I value at UE 1 from RRH 2 is equal to α_1. RRH 1 serves more than one edge UEs, so their C/I values are getting averaged in the cloud resulting in three total C/I vectors, the same as the number of the example's RRHs. Then, the values in every vector are sorted in ascending order, are then combined in the C/I matrix ($\boldsymbol{I}_M$) and the values of the first row are compared with each other. Here, we assumed that the smaller values of each vector are $\frac{\alpha_2+b_2}{2}$, c_1 and d_2 respectively. Assuming that $c_1 < d_2 < \frac{\alpha_2+b_2}{2}$, the first coalition pair to be tested is RRH 2 with RRH 1, then RRH 3 with RRH 2 and finally RRH 1 with RRH 3. Finally, the flowchart of the algorithm is depicted in Fig. 2.

The merging and splitting operations improve each RRH's payoff via Pareto order, meaning that the total utility increases in each step of the algorithm via Pareto dominance. Thus,

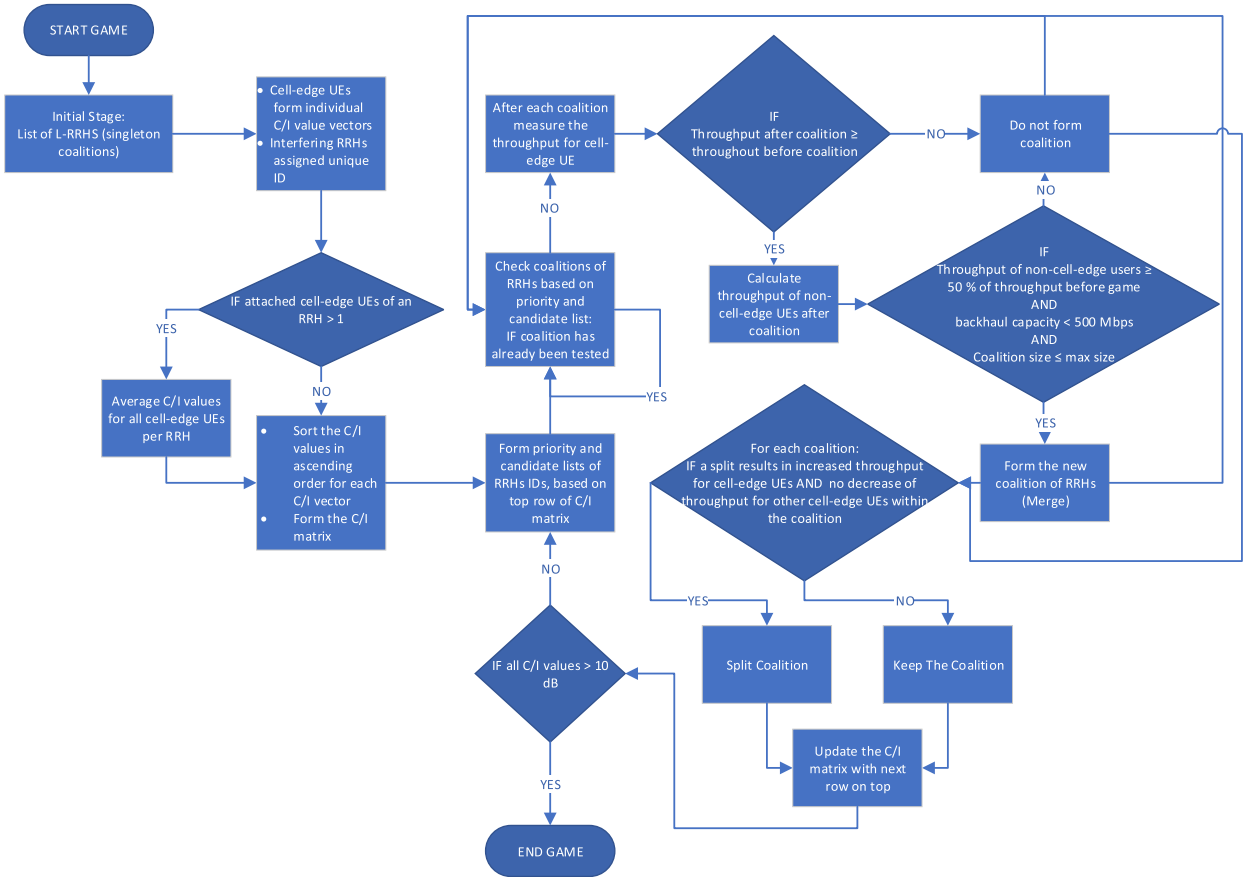

FIGURE 2. Flowchart of the proposed coalition formation algorithm.

the final outcome is result of a stable final partition where no RRH has an incentive to merge or split. Also, the proposed algorithm converges to a final stable partition on finite number of steps as the number of players is finite and every merge or split leads to Pareto improvement [35].

Finally, the C/I threshold ensures a reduced number of iterations, as only the stronger interferers of each RRH are taken into account. This means that exhaustive search is avoided and the complexity order of our proposed algorithm is $O(L_n)$, where L_n is the average number of neighbouring RRHs that create significant interference to each RRH.

VI. SIMULATION SETUP

A Cloud-RAN based small cell network consisting of 7 RRHs, placed on top of various buildings inside the University of Patras (UPAT) campus, was considered, as shown in Fig. 3. The simulations were run on the Vienna LTE-A Downlink System Level Simulator [36] and our proposed coalition formation algorithm was applied to form the most beneficial clusters for the network performance. The effective SINR threshold, which determines whether a user will be considered edge or non-edge, was set at 3 dB.

At the initial state of the simulation, where JT-CoMP and our proposed coalition formation algorithm were not activated, each RRH was set to serve 5 UEs each, accounting for a total of 35 UEs in the network. Each RRH forms a small cell, is assumed to have omnidirectional coverage and is equipped with two antennas, whilst every UE is equipped with 2 receive antennas. A carrier frequency of 2.14 GHz and a transmission power of 1 Watt was assumed. Also, the Typical Urban (TU) PDP profile was used for the computation of the small-scale parameters. Finally, each RRH had 20 MHz of available bandwidth, resulting into 100 RBs available to allocate at every TTI, according to the LTE-A specifications. These system-level simulation parameters are summarized in Table 1.

As for the algorithm's settings, a backhaul capacity threshold of 500 Mb/s and a maximum coalition size of 4 RRHs is assumed. The C/I threshold was set at 10 dB. The C/I threshold was set at a high value to account for the randomness of the UE positions. For example, an edge user, based on its position in the cell, might receive high interference from an RRH, resulting in a low individual C/I value, while another edge user might receive low interference, resulting in a high individual C/I value. The cloud averages the edge UEs' C/I values to represent the interference that all the edge UEs of an RRH receive, so in the case that the averaged C/I value is high and the C/I threshold is low, a coalition between the serving RRH and an RRH that creates severe interference for an edge UE might not be examined.

TABLE 1. Simulation parameters.

Parameter description	Value
Carrier frequency	2.14 GHz
Num. of RRHs	7
Num. of UEs per RRH	5
Inter-RRH distance	varied
Transmit power	1 Watt
Transmitter height	varied
Receiver height	1.5 meters
Antenna gain pattern	Omni-directional
Max Tx antenna gain	17 dBi
Rx antenna gain	0 dBi
Number of Tx antennas	2
Number of Rx antennas	2
LTE transmission mode	CLSM
Channel model	Typical Urban
Shadow fading type	Claussen
Receiver type	MMSE
Feedback delay	1 TTI
Bandwidth	20 MHz
Receiver noise figure	9 dB
Thermal noise density	-174 dBm/Hz

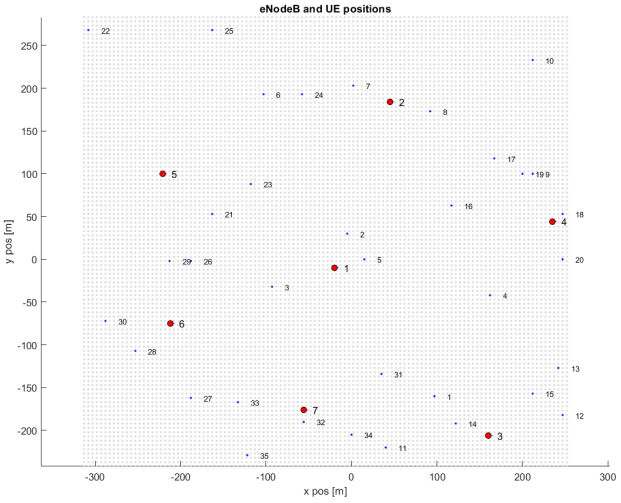

FIGURE 3. Network topology.

Our research focuses on examining the following three use cases:

1) Physical Layer Deterministic Simulation - TruNET Integration:
One of the disadvantages of system level simulators, is the use of empirical models to determine the large and small-scale propagation parameters [37]. Their use undermines the simulation scenario versatility, as topology specific scenarios are impossible to be analyzed accurately. In order to overcome this issue, we integrated *TruNET wireless*, a physical layer fully deterministic simulator with *Vienna*, a System Level simulator. TruNET is a 3D wireless network planning tool which provides a wide range of physical layer parameters as outputs using its realistic ray-tracing analysis [38]. The integration of TruNET in Vienna LTE-A Downlink System Level Simulator makes possible the use of an accurate path loss and shadowing map, thus, when the integration is active, these parameters are imported directly from the tool. In this use case, the aim is to compare the simulator's results, in terms of achievable throughput for the edge users, with and without the integration, with and without CoMP. Figure 4 depicts a snapshot of the network topology, similarly to Figure 3, combined with a much more realistic mapping of the received signal strength values per location (radiomap) that TruNET is providing for the study area (UPAT environment).

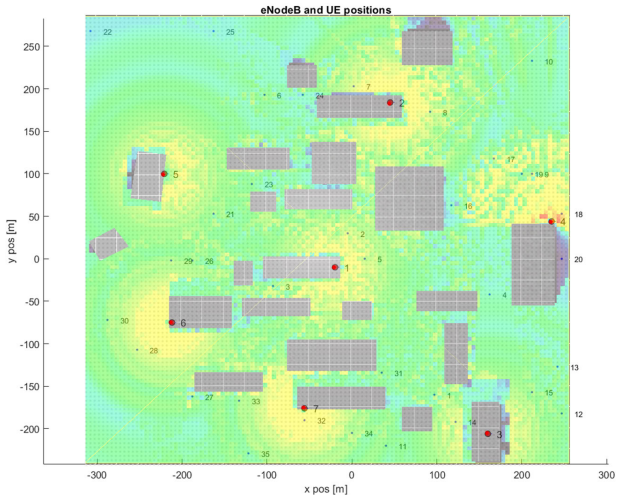

FIGURE 4. Network topology with received power mapping.

2) Application Driven Decision Making:
Until this point, the distinction between edge or non-edge UEs was made entirely by comparing their effective SINR value with a predetermined effective SINR threshold. In modern wireless networks, many applications are high demanding in terms of needed throughput, meaning that even a non-edge UE is not guaranteed to be able to carry them out efficiently and consistently if its allocated resources are not enough. To address this problem, a new condition was added in our coalition formation algorithm, where a UE can be considered edge if its throughput in the previous TTI is not sufficient for its selected application (at each simulation run, each UE's application is randomly selected). A possible drawback in this use case is that the overall edge UE percentage in the network may become extremely high, preventing the clustering of any two or more transmission points, as it will be difficult to satisfy the algorithm's conditions. The application classes considered in our research are presented in Table 2.
3) User Mobility Case:
Wireless networks in general are dynamic systems, as the wireless conditions and the factors that affect them (e.g. fading, UE positions etc.) are constantly changing. This means that when the UEs are moving, they may change status (edge from non-edge and vice

TABLE 2. Application classes.

Application Classes	Throughput Requirements (Mb/s)
Class A: Internet Browsing	0.5
Class B: Video Call	1.5
Class C: Social Media	3
Class D: HD video streaming	5

versa), or multiple handovers may occur. This may create some imbalance problems for the system, as some RRHs and clusters will have to schedule and serve a huge amount of resource hungry edge users. Our algorithm must be able to efficiently and rapidly operate its merging and splitting functionalities in order to effectively adapt to these changes and ensure adequate QoS for all the network's UEs. To make this possible, a set of new rules must be introduced in our proposed algorithm compared to the algorithm proposed in [10], [11]:

- When a handover for the moving UE occurs or its edge status changes, the proposed coalition formation algorithm is reactivated.
- If a handover or an edge status change for the moving UE occurs while the algorithm is already running, the coalition formation algorithm ignores these events.

In this use case, the throughput, the effective SINR, the serving RRH(s) and the edge status of a moving UE will be studied as it is moving with a speed of 100 km/h in a straight line, between two predetermined points.

A total of 100 simulations for every examined case were run in order to get more accurate and reliable results. A conventional case for JT-CoMP deployment, i.e. JT-CoMP with static clustering based on distance, was not examined for the first two cases, as it was presented and analyzed in [11]. However, it was considered in the user mobility case to examine how the proposed JT-CoMP scheme with our coalition formation algorithm performs against it in a scenario where multiple handovers and status changes occur. Moreover, for all the examined use cases, clustering of the transmission points based on the greedy clustering algorithm proposed in [30] is also examined. Based on this algorithm, each time, starting from a random RRH, coalitions are formed, until their size reaches the predefined max coalition size which is the same as in our proposed coalition formation game. The greedy algorithm's goal is to form coalitions which maximize condition (13), i.e. maximize the sum-throughput of all the edge UEs that are attached to the coalition's RRHs. This is a conscious choice to examine whether our proposed scheme provides the most consistent improvements in edge UE throughput as, in the greedy clustering case, possible individual throughput decreases for the edge UEs due to resource scarcity are not considered.

The scenario were JT-CoMP and our proposed coalition formation algorithm are activated is referred to as game JT-CoMP case, while the scenario where JT-CoMP is inactive

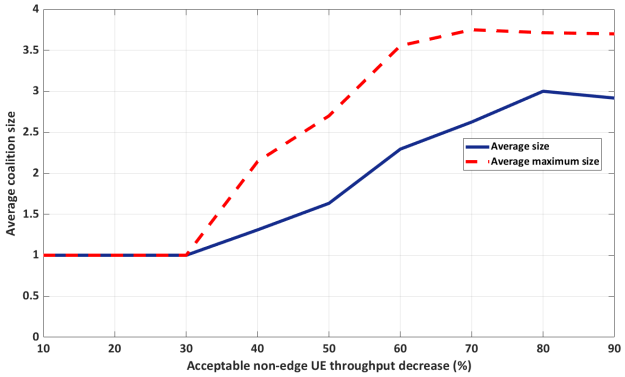

FIGURE 5. Average and average maximum coalition sizes versus the acceptable non-edge UE throughput decrease when the proposed coalition formation game is activated.

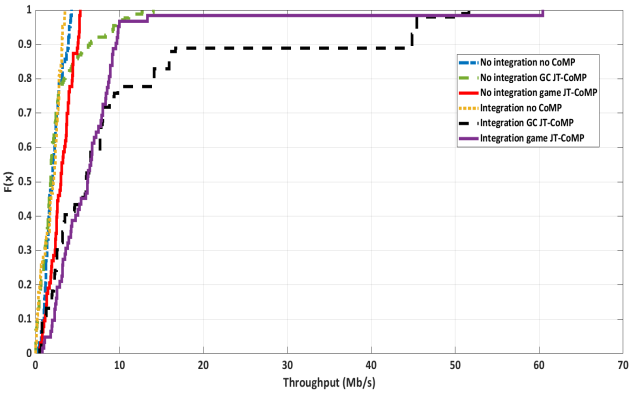

FIGURE 6. CDFs of edge UE throughput when the integration is active vs when it is inactive (homogeneous UEs).

is referred to as no CoMP case. Finally, the scenario where JT-CoMP is deployed and the clustering is made via the greedy clustering algorithm presented in [30] is referred to as GC JT-CoMP case.

To determine an appropriate value for the acceptable non-edge UE throughput decrease, various simulations for different values of α were run. Specifically, we run 100 simulations with no user mobility or application for values of α between 0.1 and 0.9, with a step of 0.1, and the results in terms of the average and maximum coalition size are depicted in Fig. 5. Based on Fig. 5, the formation of coalitions for values of α less or equal to 0.3 is impossible. Therefore, we chose the lowest value that guarantees a balance of minimum non-edge UE throughput decrease and a satisfying average and max coalition size. This value is $\alpha = 0.5$ which means that when our proposed coalition formation game is activated, a coalition between RRHs can be formed when it does not result in a throughput reduction more than 50% for any non-edge UE.

VII. RESULTS

In this section, we present all the simulation results for the three examined use cases. As mentioned in the second use case, all the UEs have been assigned a random application.

If their chosen application is a decisive factor of their status, we refer to them as heterogeneous users, otherwise they are called homogeneous users. In Figures 6-11 we examine and compare a combination of the first two use cases, while Figures 12-13 present the results of the third use case.

Fig. 6 depicts the CDF of the edge UE throughput when the TruNET integration is active or inactive, for game JT-CoMP, GC JT-CoMP and no CoMP cases, when the users are considered homogeneous and immobile. As it can be observed, for the no CoMP and both JT-CoMP scenarios, the corresponding edge UE throughput values are completely different in both the inactive integration and active integration cases, showcasing the vast difference in the computation of the channel parameters between deterministic and empirical models. An example that demonstrates even more clearly the accuracy gain that the use of physical parameters from TruNET wireless gives, is the throughput of UE 20 from Fig. 4. Specifically, UE 20 presents zero throughput value in all the simulation runs that the no CoMP integration case is considered, while in the non-integration no CoMP case, its throughput is 13.7752 Mb/s on average. This difference validates TruNET's accuracy and reliability as the empirical propagation models in Vienna LTE-A Downlink System Level Simulator do not consider unique environmental conditions that affect the wireless links. In this particular case, zero throughput for UE 20 is caused by a building obstruction and high interference from other RRHs, resulting into poor wireless channel conditions between the UE and its serving RRH and high BLER. Moreover, the JT-CoMP's gain in the edge UE throughput is apparent for both game JT-CoMP and GC JT-CoMP cases compared to the no CoMP scenario. When JT-CoMP is activated, interferers become transmitters, resulting in a huge increase of their throughput. However, for the GC JT-CoMP scenario, resource scarcity and its disregard for individual UE performance, which leads to incautious clustering of RRHs, resulted in decreased throughput for some UEs compared even to the no CoMP scenario for both the active integration and inactive integration cases.

Fig. 7 depicts the CDF of the edge UE throughput when the UEs are considered heterogeneous for all the aforementioned examined cases. The same conclusions such as for Fig. 6 can be extracted. The difference in edge UE throughput when TruNET is used in the channel modeling is apparent and the gains of JT-CoMP are more emphasized. Furthermore, the inclusion of heterogeneous UEs exposes even more the performance inconsistencies of the GC JT-CoMP scenario, for both the integration and no integration cases, as the more edge UEs in the network, the more cautious the clustering needs to be for JT-CoMP to provide throughput gains for every edge UE. For all cases, in both Fig. 6 and Fig. 7, greedy clustering gives the highest average edge UE throughput value but many UEs suffer even from thoughput reductions compared to the no CoMP scenario. Our proposed game JT-CoMP scheme provides the most consistent results, guaranteeing increase in edge UE throughput without decreasing the non-edge UEs' throughput severely.

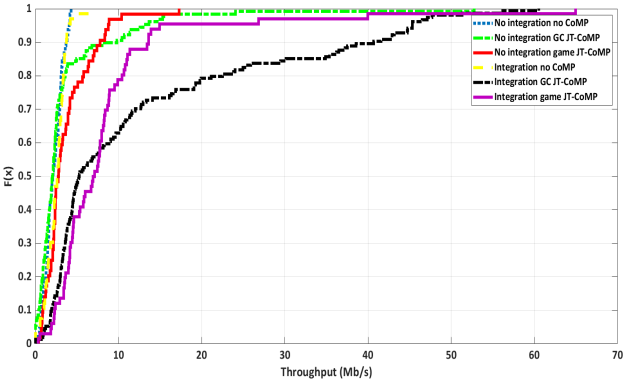

FIGURE 7. CDFs of edge UE throughput when the integration is active vs when it is inactive (heterogeneous UEs).

Fig. 8 depicts the CDF of the edge UE throughput when the UEs are considered homogeneous versus the case that the UEs are considered heterogeneous for both non-CoMP and game JT-CoMP cases, when the integration is activated. The GC JT-CoMP scenario is not examined, as we focus on the difference between these two cases in terms of edge UE throughput. The activation of JT-CoMP along with the proposed coalition formation algorithm resulted in huge throughput gains for some UEs for both homogeneous and heterogeneous user cases. The user heterogeneity results into a bigger percentage of edge UEs in the network, meaning that more UEs have a chance to increase their throughput through JT-CoMP. However, the formation of big clusters in the system is more difficult in this case as the resource scarcity may prevent edge UEs to increase their throughput and non-edge UEs to avoid theirs not to be decreased over the determined threshold, which could prohibit our proposed algorithm to form a potential cluster. This results in smaller throughput gains via the proposed scheme for some edge UEs, as it can be shown in Fig. 8.

Fig. 9, where the same cases are examined but the integration is disabled, presents more modest results, as the throughput difference between the non-CoMP and game JT-CoMP cases is relatively small due to using only the empirical models of Vienna LTE-A Downlink System Level Simulator. Again, some UEs in the heterogeneous case, improve vastly their throughput compared to the homogeneous case, while some others present lower values than the homogeneous case, which is an immediate result of the size of the formed clusters and/or the resource scarcity.

Fig. 10 presents the different average edge to non-edge UE throughput ratio for all the examined cases. As expected, when the integration is active, this ratio is different than the no integration case. Table 3 provides the average throughput values for edge and non-edge UEs for all the cases. The average throughput ratio for almost all the homogeneous cases is less than the heterogeneous cases because many UEs normally considered non-edge (i.e. UEs with higher throughput value in comparison), are included in the latter, increasing the average throughput value. Table 3 confirms that there was

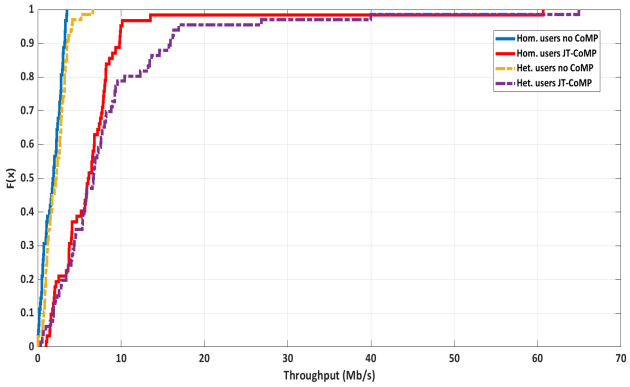

FIGURE 8. CDFs of homogeneous edge UE throughput vs heterogeneous edge UE throughput (active integration).

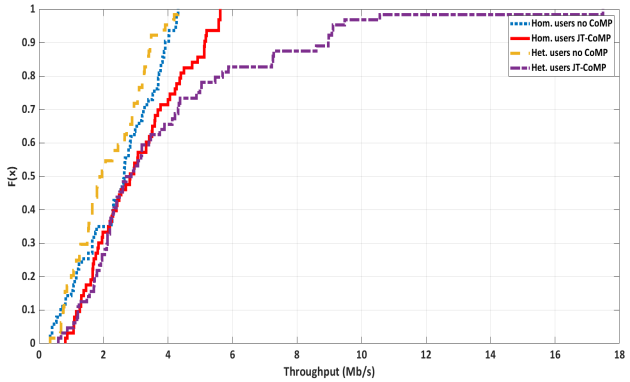

FIGURE 9. CDFs of homogeneous edge UE throughput vs heterogeneous edge UE throughput (deactivated integration).

TABLE 3. Average UE throughput values per case.

	non-edge (Mb/s)	edge (Mb/s)
no CoMP no integration hom.	16.3314	1.9402
no CoMP no integration het.	16.9717	1.9641
no CoMP integration hom.	6.7407	2.3123
no CoMP integration het.	7.2472	2.8252
game JT-CoMP no integr. hom.	10.6892	2.9621
game JT-CoMP no integr. het.	10.7182	4.4847
game JT-CoMP integr. hom.	4.6612	10.7723
game JT-CoMP integr. het.	4.5233	12.8239

no case where the average throughput of the non-edge UEs is reduced more than 50% when game JT-CoMP is active, as the individual reduction of non-edge UE throughput is considered in our formulated coalition formation game. Also, it is notable that the average non-edge UE throughput is significantly lower when the integration is active which again proves the inaccuracy of the employed empirical models of the Vienna LTE-A Downlink System Level Simulator for specific propagation topologies. Finally, an enormous increase is noticed for the edge UEs' average throughput when the integration and game JT-CoMP are active, which ensures a better performance balance for all the network devices since the average non-edge UE throughput is not significantly decreased.

TABLE 4. Average edge UE throughput per application class (allocation 6).

	Class A	Class B	Class C	Class D
no CoMP hom.	2.8346	2.3025	1.8870	3.1134
no CoMP het.	2.8346	2.4262	1.8903	3.2548
game JT-CoMP hom.	6.5163	3.3874	5.3674	11.5549
game JT-CoMP het.	6.5347	2.7333	5.2871	17.1366

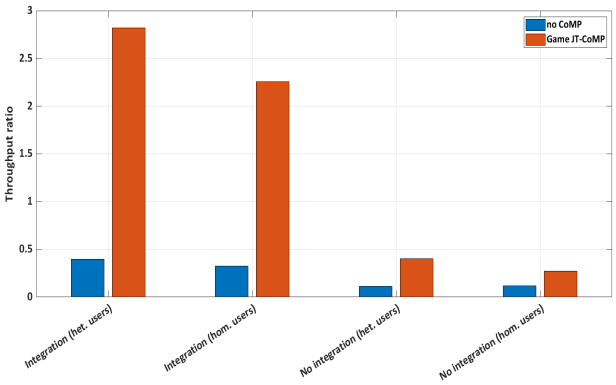

FIGURE 10. Average edge to non-edge UE throughput ratio for all examined cases.

TABLE 5. Allocation preferences.

	Class A	Class B	Class C	Class D
Allocation 1 (%)	80	10	5	5
Allocation 2 (%)	25	25	25	25
Allocation 3 (%)	5	5	10	80
Allocation 4 (%)	10	20	60	10
Allocation 5 (%)	10	60	15	15
Allocation 6 (%)	30	10	40	30

In Table 4 and Fig. 11 we examine the behavior of the edge UEs' throughput for different allocation preferences of the application classes. Table 5 presents the different preference allocations that were tested, while Table 4 presents the average throughput for all the application classes' edge UEs when allocation 6 was chosen and the integration is active. For all the cases, when game JT-CoMP is applied, the average throughput is higher than the required one. Especially for the most demanding application class, class D, the heterogeneous case provided the highest average throughput. Also, it is notable that the average throughput of the edge UEs that carry out the application class B, when the heterogeneous case was considered, presents the smallest value amongst the cases that CoMP was applied as a result of the resource scarcity.

Fig. 11 describes the average heterogeneous edge UE throughput for the different allocation preferences presented in Table 5. When different application class allocations are selected, different number of UEs perform the corresponding application. When the probability for an application to be selected increases, more UEs will perform this application and if their throughput is lower than required, they will become edge. Also, the basic criterion for determining whether a user is edge or not is still considered, so, many UEs with low demanding applications would get anywise

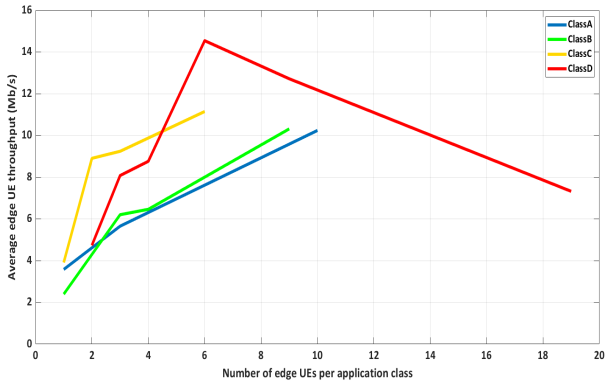

FIGURE 11. Average edge UE throughput for different allocation preferences.

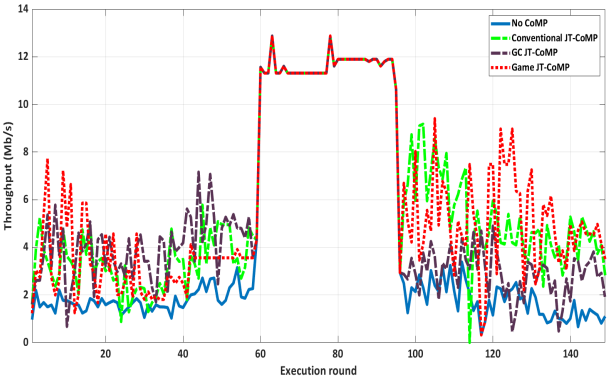

FIGURE 12. Average moving UE throughput per 10 TTIs.

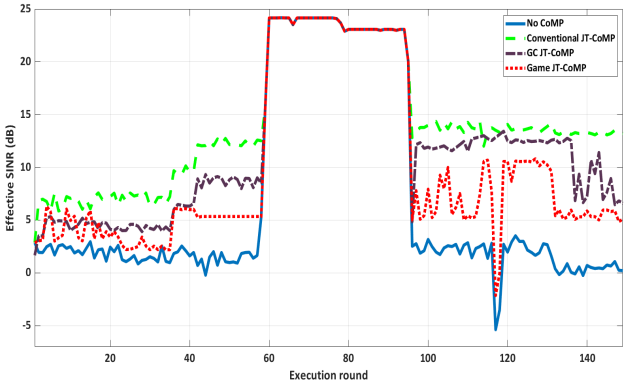

FIGURE 13. Average moving UE effective SINR per 10 TTIs.

improved throughput values. For all the cases, the more edge UEs perform an application, the probability of an edge UE that would present via JT-CoMP a large throughput, increases. This explains the upturn for the curves of classes A, B and C. For class D, when allocation preference 2 of Table 5 is selected, a saturation point is noticed, because if this demanding application class is selected by many UEs, it is possible that many of them will be classified as edge UEs. This means that the network will be densely populated by edge UEs, resulting in a point beyond which the available resources are not enough to satisfy the users' throughput needs. Results from Fig. 8, Fig. 9 and Fig. 11 indicate that while game JT-CoMP will always provide throughput gains, a large percentage of edge UEs in the network may result in moderate to insignificant throughput gains compared to the homogeneous edge UE case.

As for the third use case, Fig. 12 and Fig. 13 depict the average per 10 TTIs throughput and effective SINR of the selected moving UE (UE 4 in Fig. 3 and Fig. 4) respectively, when game JT-CoMP is activated versus the conventional JT-CoMP, GC JT-CoMP and no CoMP cases. We assume that 10 TTIs correspond to an execution round and that the integration is active. The UE moved for 1490 TTIs from coordinates $x_1 = 162\text{m}, y_1 = -42\text{m}$ to $x_2 = 162\text{m}, y_2 = -0.6\text{m}$. Table 6 provides a detailed description of the number of serving RRHs, the UE's status and the execution rounds that the proposed algorithm was activated throughout the user's movement. For the conventional JT-CoMP case, we assumed two static clusters based on inter-RRH distance, where the first one is consisted of RRHs 1-4 and the second one includes RRHs 5-7. These clusters were chosen in a way that the moving UE was always served by at least the same amount of RRHs compared to the game JT-CoMP case. Table 7 shows the serving RRHs for the moving user when the conventional JT-CoMP case was considered. For the game JT-CoMP case, at the first execution round, the moving UE acquired its edge status and the proposed algorithm activated until execution round 28. After a handover during execution round 33, the UE was momentarily served by one RRH before the proposed coalition formation algorithm was activated again and the UE was served by two cooperating RRHs. At execution round 58 the UE was considered non-edge, so it was not served by a coalition. The user regained its edge status at execution round 96, the coalition formation algorithm was reactivated and the user was served by a coalition via JT-CoMP. Again, after a handover at execution round 116, our proposed algorithm was activated again and this time a larger coalition was formed to serve the moving UE. By observing Fig. 12 and Fig. 13, it is clear that game JT-CoMP consistently benefited the moving UE's throughput throughout its movement, compared to the no CoMP case, and was able to quickly assign cooperating RRHs for its service, despite handovers and status changes. As expected, the conventional JT-CoMP case benefited the moving UE the most in terms of effective SINR. However, the cooperating RRHs had to schedule RBs to a large number of users due to large cluster size which did not allowed an equivalent increase in the moving user's throughput. This was reflected in several execution rounds where the conventional JT-CoMP case was outperformed by the game JT-CoMP case. Furthermore, there were execution rounds that the moving user's throughput was lower even than the no CoMP case due to RB scarcity. In terms of effective SINR, the GC JT-CoMP scenario provided the second best values but again, resource scarcity and the randomness of coalitions that emerge through the greedy clustering algorithm did not result in an equivalent increase in the user's throughput. Moreover, the GC JT-CoMP

TABLE 6. Description of moving UE's status, serving RRH(s) and the proposed algorithm's actions for all the runs.

Execution Round(s)	Serving RRH(s)	Algorithm	Status
1	1	inactive	edge
2-28	1,4	active	edge
29-33	1,4	inactive	edge
33 + 9 TTIs (Handover)	5	inactive	edge
34-42	5,2	active	edge
43-57	5,2	inactive	edge
58-95	5	inactive	non-edge
96-113	5,2	active	edge
113-116	5,2	inactive	edge
116 + 9 TTIs (Handover)	4	inactive	edge
117-129	4,1,5,2	active	edge
129-149	4,1,5,2	inactive	edge

TABLE 7. Description of moving UE's status and serving RRH(s) for the conventional JT-CoMP case.

Execution Round(s)	Serving RRH(s)	Status
1	1	edge
2-33	1,2,3,4	edge
33 + 9 TTIs (Handover)	5	edge
34-57	5,6,7	edge
58-95	5	non-edge
96-116	5,6,7	edge
116 + 9 TTIs (Handover)	4	edge
117-149	4,1,2,3	edge

scenario gave the most inconsistent results, since the moving UE's throughput got high values in many execution rounds, and throughput even below the no CoMP case in others.

It is noticeable that through the proposed coalition formation algorithm the moving user was not served by the RRHs closest to each other as it can be seen e.g. for execution rounds 117-149, where RRH 5 served also the moving user. This validates the proposed scheme's intelligence in clustering decisions, since it was able to form the most beneficial coalitions of RRHs to serve the edge UEs, regardless of the distance between them. Furthermore, the proposed scheme provided the most consistent throughput improvements, while guaranteeing a moderate decrease in throughput for all non-edge UEs.

Flunctuations of the UE's throughput can be observed in Fig. 12 when the proposed algorithm is activated after a handover or status change, as the algorithm tried different coalitions where some of them did not benefited the moving UE's throughput. However, as JT-CoMP was applied, the moving UE's effective SINR was improved for all the execution rounds compared to the no CoMP case.

From the results of Fig. 12, Fig. 13 and Table 6, it is clear that in a realistically modelled/real environment, and especially in an urban one, it is not guaranteed that a UE will be served by the closest transmission point, as many more propagation parameters affect the quality of the wireless links besides distance. Also, in less than 50 meters covered distance, two handovers happened, confirming the distinctiveness of an urban small cell propagation environment. Hardware limitations prevented the monitoring of the UE's behavior for a greater covered distance.

VIII. CONCLUSION

The JT-CoMP technique is an extremely important scheme for modern wireless networks as the network densification can increase severely the intercell interference for mobile users in the cell edges. Moreover, as it is not enough to increase a user's SINR to guarantee better performance and the available resources are limited, the clustering of transmission points for the JT-CoMP implementation must be cautious for a fair and reliable service of all the network's users and the satisfaction of backhaul capacity constraints.

In this article, a coalition formation game was formulated to cluster the RRHs in a C-RAN based small cell scenario where the user mobility is a factor and different users have different throughput needs, depending on their application. To accurately study our proposed coalition formation method and JT-CoMP's impact, simulations using output imported from a fully deterministic physical layer planning tool were run and compared to a case that empirical models were considered. Results verified that the realistic modeling provides different results compared to simulations with empirical models and that our proposed self-organization scheme was able to provide consistent throughput gains for all the examined cases. Furthermore, it was demonstrated that when the number of edge users becomes large, the throughput gains of our proposed scheme can be limited.

REFERENCES

[1] P. Popovski, "Ultra-reliable communication in 5G wireless systems," in *Proc. 1st Int. Conf. 5G Ubiquitous Connectivity*, Nov. 2014, pp. 146–151.
[2] P. Pirinen, "A brief overview of 5G research activities," in *Proc. 1st Int. Conf. 5G Ubiquitous Connectivity*, Nov. 2014, pp. 17–22.
[3] N. Bhushan, J. Li, D. Malladi, R. Gilmore, D. Brenner, A. Damnjanovic, R. Sukhavasi, C. Patel, and S. Geirhofer, "Network densification: The dominant theme for wireless evolution into 5G," *IEEE Commun. Mag.*, vol. 52, no. 2, pp. 82–89, Feb. 2014.
[4] S. Mumtaz, K. M. S. Huq, J. Rodriguez, S. Ghosh, E. E. Ugwuanyi, M. Iqbal, T. Dagiuklas, S. Stavrou, L. Kanaris, I. D. Politis, A. Lykourgiotis, T. Chrysikos, P. Nakou, and P. Georgakopoulos, "Self-organization towards reduced cost and energy per bit for future emerging radio technologies–SONNET," in *Proc. IEEE Globecom Workshops (GC Wkshps)*, Dec. 2017, pp. 1–6.
[5] J. Rodriguez, A. Radwan, C. Barbosa, F. H. P. Fitzek, R. A. Abd-Alhameed, J. M. Noras, S. M. R. Jones, I. Politis, P. Galiotos, G. Schulte, A. Rayit, M. Sousa, R. Alheiro, X. Gelabert, and G. P. Koudouridis, "SECRET—Secure network coding for reduced energy next generation mobile small cells: A European training network in wireless communications and networking for 5G," in *Proc. Internet Technol. Appl. (ITA)*, Wrexham, U.K., Sep. 2017, pp. 329–333.
[6] A. Checko, H. L. Christiansen, Y. Yan, L. Scolari, G. Kardaras, M. S. Berger, and L. Dittmann, "Cloud RAN for mobile networks—A technology overview," *IEEE Commun. Surveys Tuts.*, vol. 17, no. 1, pp. 405–426, 1st Quart., 2015.
[7] *C-RAN: The Road Towards Green RAN, White Paper, Ver. 2.5*, China Mobile Res. Inst., Beijing, China, 2011.
[8] R. Irmer, H. Droste, P. Marsch, M. Grieger, G. Fettweis, S. Brueck, H.-P. Mayer, L. Thiele, and V. Jungnickel, "Coordinated multipoint: Concepts, performance, and field trial results," *IEEE Commun. Mag.*, vol. 49, no. 2, pp. 102–111, Feb. 2011.
[9] V. Jungnickel, K. Manolakis, W. Zirwas, B. Panzner, V. Braun, M. Lossow, M. Sternad, R. Apelfrojd, and T. Svensson, "The role of small cells, coordinated multipoint, and massive MIMO in 5G," *IEEE Commun. Mag.*, vol. 52, no. 5, pp. 44–51, May 2014.

[10] P. Georgakopoulos, T. Akhtar, I. Politis, C. Tselios, E. Markakis, and S. Kotsopoulos, "Coordination multipoint enabled small cells for coalition-game-based radio resource management," *IEEE Netw.*, vol. 33, no. 4, pp. 63–69, Jul. 2019.

[11] P. Georgakopoulos, T. Akhtar, and S. Kotsopoulos, "On game theory-based coordination schemes for mobile small cells," in *Proc. IEEE 24th Int. Workshop Comput. Aided Model. Design Commun. Links Netw. (CAMAD)*, Sep. 2019, pp. 1–5.

[12] Z. Han and H. V. Poor, "Coalition games with cooperative transmission: A cure for the curse of boundary nodes in selfish packet-forwarding wireless networks," *IEEE Trans. Commun.*, vol. 57, no. 1, pp. 203–213, Jan. 2009.

[13] S. Shamai and B. M. Zaidel, "Enhancing the cellular downlink capacity via co-processing at the transmitting end," in *Proc. IEEE VTS 53rd Veh. Technol. Conf., Spring*, vol. 3, May 2001, pp. 1745–1749.

[14] H. Zhang and H. Dai, "Cochannel interference mitigation and cooperative processing in downlink multicell multiuser MIMO networks," *EURASIP J. Wireless Commun. Netw.*, vol. 2004, no. 2, Dec. 2004, Art. no. 202654.

[15] V. Jungnickel, L. Thiele, T. Wirth, T. Haustein, S. Schiffermuller, A. Forck, S. Wahls, S. Jaeckel, S. Schubert, H. Gabler, C. Juchems, F. Luhn, R. Zavrtak, H. Droste, G. Kadel, W. Kreher, J. Mueller, W. Stoermer, and G. Wannemacher, "Coordinated multipoint trials in the downlink," in *Proc. IEEE Globecom Workshops*, Nov. 2009, pp. 1–7.

[16] D. Lee, H. Seo, B. Clerckx, E. Hardouin, D. Mazzarese, S. Nagata, and K. Sayana, "Coordinated multipoint transmission and reception in LTE-advanced: Deployment scenarios and operational challenges," *IEEE Commun. Mag.*, vol. 50, no. 2, pp. 148–155, Feb. 2012.

[17] S. S. Ali and N. Saxena, "A novel static clustering approach for CoMP," in *Proc. 7th Int. Conf. Comput. Converg. Technol. (ICCCT)*, Dec. 2012, pp. 757–762.

[18] P. Marsch and G. Fettweis, "Static clustering for cooperative multi-point (CoMP) in mobile communications," in *Proc. IEEE Int. Conf. Commun. (ICC)*, Jun. 2011, pp. 1–6.

[19] H. Shimodaira, G. K. Tran, K. Sakaguchi, K. Araki, S. Nanba, and S. Konishi, "Diamond cellular network—Optimal combination of small power basestations and CoMP cellular networks—," *IEICE Trans. Commun.*, vol. 99, no. 4, pp. 917–927, 2016.

[20] S. Feng, W. Feng, H. Mao, and J. Lu, "Overlapped clustering for comp transmissions in massively dense wireless networks," in *Proc. IEEE Int. Conf. Commun. Syst.*, Nov. 2014, pp. 308–312.

[21] J.-M. Moon and D.-H. Cho, "Formation of cooperative cluster for coordinated transmission in multi-cell wireless networks," in *Proc. IEEE 10th Consum. Commun. Netw. Conf. (CCNC)*, Jan. 2013, pp. 528–533.

[22] C. Choi, L. Scalia, T. Biermann, and S. Mizuta, "Coordinated multipoint multiuser-MIMO transmissions over backhaul-constrained mobile access networks," in *Proc. IEEE 22nd Int. Symp. Pers., Indoor Mobile Radio Commun.*, Sep. 2011, pp. 1336–1340.

[23] M. U. Aminu, J. Kaleva, and A. Tolli, "Dynamic clustering for max-min fairness with joint processing CoMP," in *Proc. IEEE 27th Annu. Int. Symp. Pers., Indoor, Mobile Radio Commun. (PIMRC)*, Sep. 2016, pp. 1–5.

[24] A. Daher, M. Coupechoux, P. Godlewski, P. Ngouat, and P. Minot, "A dynamic clustering algorithm for multi-point transmissions in mission-critical communications," *IEEE Trans. Wireless Commun.*, vol. 19, no. 7, pp. 4934–4946, Jul. 2020.

[25] S. Bassoy, M. Jaber, M. A. Imran, and P. Xiao, "Load aware self-organising user-centric dynamic CoMP clustering for 5G networks," *IEEE Access*, vol. 4, pp. 2895–2906, 2016.

[26] S. Guruacharya, D. Niyato, M. Bennis, and D. I. Kim, "Dynamic coalition formation for network MIMO in small cell networks," *IEEE Trans. Wireless Commun.*, vol. 12, no. 10, pp. 5360–5372, Oct. 2013.

[27] S.-C. Zhan and D. Niyato, "A coalition formation game for remote radio head cooperation in cloud radio access network," *IEEE Trans. Veh. Technol.*, vol. 66, no. 2, pp. 1723–1738, Feb. 2017.

[28] M. Ahmed, M. Peng, M. Abana, S. Yan, and C. Wang, "Interference coordination in heterogeneous small-cell networks: A coalition formation game approach," *IEEE Syst. J.*, vol. 12, no. 1, pp. 604–615, Mar. 2018.

[29] S. Bassoy, M. A. Imran, S. Yang, and R. Tafazolli, "A load-aware clustering model for coordinated transmission in future wireless networks," *IEEE Access*, vol. 7, pp. 92693–92708, 2019.

[30] F. Guidolin, L. Badia, and M. Zorzi, "A distributed clustering algorithm for coordinated multipoint in LTE networks," *IEEE Wireless Commun. Lett.*, vol. 3, no. 5, pp. 517–520, Oct. 2014.

[31] *Technical Specification Group Radio Access Network, Evolved Universal Terrestrial Radio Access (E-UTRA), Physical Channels and Modulation (Release 11)*, document TS 36.211, 3GPP, Dec. 2012.

[32] A. Alexiou *et al.*, "IST-2003-507581 WINNER D2. 7 ver 1.0 assessment of advanced beamforming and MIMO technologies," Inf. Soc. Technol., Brussels, Belgium, Tech. Rep., 2005.

[33] M. Taranetz, T. Blazek, T. Kropfreiter, M. K. Müller, S. Schwarz, and M. Rupp, "Runtime precoding: Enabling multipoint transmission in LTE-advanced system-level simulations," *IEEE Access*, vol. 3, pp. 725–736, 2015.

[34] V. Jungnickel, K. Manolakis, S. Jaeckel, M. Lossow, P. Farkas, M. Schlosser, and V. Braun, "Backhaul requirements for inter-site cooperation in heterogeneous LTE-advanced networks," in *Proc. IEEE Int. Conf. Commun. Workshops (ICC)*, Jun. 2013, pp. 905–910.

[35] W. Saad, Z. Han, M. Debbah, A. Hjorungnes, and T. Basar, "Coalitional game theory for communication networks," *IEEE Signal Process. Mag.*, vol. 26, no. 5, pp. 77–97, Sep. 2009.

[36] M. Rupp, S. Schwarz, and M. Taranetz, *The Vienna LTE-Advanced Simulators*. Singapore: Springer, 2016.

[37] L. Kanaris, C. Sergiou, A. Kokkinis, A. Pafitis, N. Antoniou, and S. Stavrou, "On the realistic radio and network planning of IoT sensor networks," *Sensors*, vol. 19, no. 15, p. 3264, Jul. 2019.

[38] *TruNET Wireless*. Accessed: Sep. 16, 2020. [Online]. Available: http://www.fractalnetworx.com

PANAGIOTIS GEORGAKOPOULOS (Member, IEEE) received the Diploma degree from the Department of Electrical and Computer Engineering, University of Patras, Greece, in 2016. He is currently pursuing the Ph.D. degree with the Wireless Telecommunications Laboratory, University of Patras. He is currently a Marie Curie Early Stage Researcher with the Wireless Telecommunications Laboratory, University of Patras. His research interests include 5G and beyond networks, radio planning, radio resource management, and cooperative and self-organized networks.

LOIZOS KANARIS received the B.Sc. degree in aviation science from Hellenic Airforce Academy, the master's degree in business administration from Cyprus European University, and the Ph.D. degree from the Department of Electrical Engineering, Eindhoven University of Technology focusing his research work on wireless indoor and outdoor localization techniques. In the aspect of academic and research, he has leaded the Research and Development Department, Sigint Solutions Ltd., a research performing organization that develops edge of technology telecom and crisis management platforms, such as ORION and *TruNET wirelessTM*. He designed and implemented and ISO 17025 accreditation for the organization's laboratory, on low and high EMF measurement procedures. He also actively participated in numerous EU and National research projects, such as WHERE (FP7), WHERE2 (FP7) and LOCME (RPF), and SONNET (HORIZON 2020) investigating wireless positioning aspects and 5G+ cellular technologies. Finally, he has published a number of peer-reviewed publications in his research areas of interest, he has been serving as a Reviewer in a several scientific publications in the area of wireless telecom and he has been listed as an Exemplary Reviewer in the IEEE Wireless Communication Letters in 2015.

TAFSEER AKHTAR (Graduate Student Member, IEEE) received the master's degree in cyber security from the Department of Computer Engineering, National Institute of Technology of Kurukshetra, India, in 2017. He is currently an Early Stage Researcher and a Marie Curie Fellow with the Department of Electrical and Computer Engineering, University of Patras. His research interests include but are not limited to 5G small cell networks, radio resource management, game theory, distributed learning, network coded cooperation, and network security.

AKIS KOKKINIS received the B.Sc. degree in aviation science from the Hellenic Airforce Academy in Athens, with a diploma thesis in computational aerodynamics (operational navigation flight planning, including 3D radar coverage, radar prediction and visualization features), in 1998, and the Ph.D. degree from the Department of Electrical Engineering, Eindhoven University of Technology, focusing his research work on the investigation of enhanced hybrid indoor positioning algorithms. Since 2001, he has been a member of the Research and Development Department, SIGINT, as a Software Architect and a Lead Developer for several Telecommunication platforms, such as *TruNET* and *3D Ray Tracing Simulator*. Additionally, he is heavily involved in FP6, FP7, and national ICT funded projects where Sigint Solutions Ltd., carries out research work on multiple layers of the OSI protocol stack. Examples of these projects include UNITE (FP6), FUTON (FP7), WHERE (FP7), and COGEU (FP7).

STAVROS STAVROU (Member, IEEE) received the Ph.D. degree in electronic engineering from the University of Surrey, U.K. From 1997 to 2009, he was a Faculty Member with the Centre for Communication Systems Research (CCSR), University of Surrey. In 2009, he joined the Open University of Cyprus (OUC), where he established and leads the Cybersecurity and Telecommunications Research Laboratory (CTRL). He is currently the Dean of Faculty of Pure and Applied Sciences. He has been involved with the design and management of several M.Sc. academic programmes, such as *Information Systems*, *Information and Communication Systems*, *Wireless Communication Systems*, and *Computer and Network Security*. He was also responsible for designing and implementing OUC's first virtual Lab infrastructure, allowing students to remotely access any delivered virtual lab from any device. His areas of expertise cover communication networks, telecommunication systems, and cybersecurity security applications. His current research interests include different cross layer topics in the above areas. He has authored or coauthored more than 100 journal publications, book chapters, and conference proceedings publications. He has raised more than seven million euros in personal research grants (PI) from research councils, government organizations, and industrial collaborations. Some of the organizations with which he has initiated, managed and carried out work for include: EPSRC, Defence and Science Technology Laboratory (MoD, U.K.), Mobile VCE, Rolls Royce plc, Inmarsat, and others. He has also been a major contributor in a number of EU and national research projects. Some of these projects include: W (EU), SATNEX (EU), UNITE (EU), FUTON (EU), WHERE (EU), LOOP (EURPF), MOBILIA (EURPF), ICARUS (EURPF), MOTIFS (RPF), 4GOPEN (EU/RPF), WHERE 2 (EU), COGEU (EU), C2POWER (EU), LocMe (RPF), UPI(RPF), i-LocON (RPF), RFMETA(RPF), CSRC(EU), SWITCH(RPF), and FORESIGHT (EU). He has contributed towards numerous technical reports and he is the patent holder of a mobile phone jammer. He is a Fellow of the Higher Education Academy U.K., an appointed member of the executive academic board of the European Defence and Security College (ESDC) and the First elected Chairman of its Cyber Group configuration. He will be leading OUC's (CTRL's) project effort and will be contributing in multiple tasks.

ILIAS POLITIS (Member, IEEE) received the B.Sc. degree in electronic engineering from Queen Marry College London, U.K., in 2000, the M.Sc. degree in mobile and personal communications from King's College London, U.K., in 2001, and the Ph.D. degree in multimedia communications from the University of Patras, Greece, in 2009. He is currently a Senior Researcher with the Department of Digital Systems, University of Piraeus, while previous posts include a Senior Researcher with the Wireless Telecommunications Laboratory of the Electrical and Computer Engineering, University of Patras, and the School of Science and Technology, Hellenic Open University, Greece. He has been actively involved in all phases of several H2020 and FP7 framework projects. His research interests include future internet and next generation networks (5G and beyond), contextual awareness and network security, where he has published more than 90 journals and conferences.